J Mater Sci (2012) 47:440–454
DOI 10.1007/s10853-011-5819-7

Preparation of sol–gel-based nanostructured hybrid coatings; part 1: morphological and mechanical studies

B. Ramezanzadeh · M. Mohseni · A. Karbasi

Received: 31 January 2011 / Accepted: 25 July 2011 / Published online: 2 August 2011

Abstract Attempts have been made using sol–gel-based precursors to produce hybrid organic–inorganic clearcoats. To this end, a typical automotive acrylic/melamine clearcoat with tetramethyl ortosilicate (TEOS) and methacryloxy propyltrimethoxysilane (MEMO) were used to obtain nanostructured silica clusters produced in situ embedded in the polymeric matrix. Microscopic techniques including scanning electron microscope (SEM), atomic force microscope (AFM), and transmission electron microscope (TEM) were utilized to investigate the morphology of coatings. The effect of each precursor on coating mechanical properties was also studied using dynamic mechanical thermal analysis (DMTA) as well as micro and nanoindentation techniques. It was found that using TEOS and MEMO (in non-hydrolyzed state), the mechanical properties of the resulting films were negatively influenced. The decreased hardness, lower T_g and cross-linking density, and reduced elastic modulus were observed with non-hydrolyzed precursors. In addition, the phase separation of organic and inorganic domains occurred in the presence of pristine sol–gel precursors. However, using hydrolyzed precursors (HTEOS and HMEMO), the mechanical properties were notably improved. While HTEOS resulted in an increase in coating T_g, and cross-linking density as well as improved elastic modulus and hardness, HMEMO caused an increase in coating hardness but lowered coating T_g and cross-linking density.

B. Ramezanzadeh · M. Mohseni (✉) · A. Karbasi
Department of Polymer Engineering and Color Technology, Amirkabir University of Technology, P.O. Box 15875-4413, Tehran, Iran
e-mail: mmohseni@aut.ac.ir

Introduction

Basecoat/clearcoat coating systems have been utilized in automotive industries for many years. In this system, the non-pigmented clearcoat is mainly responsible for the smoothness and glossiness [1, 2]. However, these properties can be easily influenced when the system is exposed to outdoor environments such as UV irradiation, humidity, biological materials, and physical/mechanical factors [3–5].

Scratch and mar are the most important kinds of the mechanical damages and can be produced by tree branches, sharp objects such as car keys, polishing equipments, car-wash bristles etc. [1, 5]. Mar refers to the shallow (0–0.5 μm) light surface damages while scratch refers to medium to severe damages (>0.5 μm) encountered in the service life of coatings. Scratches may have plastic or fracture morphology. Fracture mode scratches due to their sharp and irregular shapes can severely scatter visible light. On the other hand, plastic mode scratches have smoother edges with a regular shape causing less light scattering and appearance changes [5–7]. Different factors such as temperature, severity of applied external load, chemical composition, and mechanical properties of a clearcoat layer can cause different types of deformation [8–10]. UV irradiation and humidity can also influence coating properties during service life. In fact, hydrolytic degradation occurs in humid condition [11, 12]. On the other hand, photo-degradation can occur when the coating is exposed to UV irradiation [5]. One of the most important but rarely reported kinds of automotive coatings degradation is the biological type. In the previous studies, effects of different kinds of biological materials as well as main parameters affecting degradation of the coatings have been reported [3, 4]. It was found that one of the naturally occurring materials such as bird

droppings, due to existence of some digestive hydrolyze enzymes (amylase and lipase) are able to catalyze the hydrolytic cleavage of the polymeric coatings. The consequence of such cleavages is the release of water soluble products from coating, leaving local etched defects on coating surface [3]. As a result, the mechanical, appearance, and anticorrosion properties of the clearcoat can be significantly affected. The effects of other natural compounds like tree gums on the clearcoats properties were also studied [4]. It was found that the pronounced influence of natural tree gum was a severe crack formation and shrinkage on fully coated systems and free film samples, respectively.

Various approaches have come into existence to improve coating resistance against these outdoor mechanical, chemical, and biological factors. Use of different types of nanoparticles e.g., SiO_2, TiO_2, and Al_2O_3 have been used for this purpose [1, 13, 14]. These nanoparticles, due to their very small sizes and high surface areas, can significantly improve the coating scratch resistance. However, there can be encountered problems using these nanoparticles with respect to the difficulties in dispersion process. Although, use of surface functionalized [13–16] particles may overcome this problem, the dispersion process still needs to be enhanced. Moreover, by incorporating these powders an increase in viscosity may be observed. So, the particles loading should be kept as low as possible to avoid this difficulty. It should also be noted that inferior particle dispersion can negatively influence the appearance and mechanical properties of coating.

Thanks to the versatile chemistry of sol–gel processing, metal oxide nanoparticles can be produced in situ using appropriate organic–inorganic precursors [17–27]. These precursors, either as network former [27], such as tetraethyl orthosilicate (TEOS) or as network modifier, such as methacryloxy propyltrimethoxysilane (MEMO) and glycidoxy propyl trimethoxysilane (GPTS), can be introduced to the main polymeric film former to obtain a so-called hybrid nanocomposite film. Little studies have been carried out on the application of this approach in automotive clearcoats resins. The overall film formation involves hydrolysis and condensation of sol–gel precursor as well as the ability of main polymeric matrix to be cross-linked through appropriate functional groups in amino-cured acrylic polyol or isocyanate-cured hydroxyl containing resins. In addition, there is likely to observe an entanglement between organic functional groups of sol–gel precursors such as acrylics in MEMO and epoxy in GPTS and the main film former. Based on such reactions, in situ silicon containing hybrid nanocomposites are accessible, enabling to obtain a mechanically reinforced system. The organic phase is responsible for the general characteristics of the films such as adhesion, flexibility, and environmental resistance of the coatings while the inorganic phase makes the film resist against mechanical damages. There are many advantages for using sol–gel method to create silica particles in a coating matrix [17–32]. The particle size and distribution can be easily tuned by controlling the parameters affecting hydrolysis and condensation reactions. An interpenetrating network can then be produced in which organic and inorganic domains have been formed in nanometer size. However, the presence of water to pursue the hydrolysis reaction may be a problem to carefully adjust the miscibility of sol–gel precursors in solvent-based coating formulations. Therefore, controlled hydrolysis and condensation reactions may prevent phase separation, otherwise different types of morphologies may be obtained [23–36].

The aim of this study is to improve the mechanical properties of a sol–gel-based acrylic/melamine automotive clearcoat. Nanostructured silicas were produced using sol–gel processing at different combinations of precursors. Effects of hydrolysis condition on morphological and mechanical behaviors of the resulting hybrid films were investigated using various analytical techniques inclusive of TEM, SEM, AFM, and nanoindentation method.

Experimental

Materials and sample preparation

The multilayered automotive coating system used in this study included a 2–3 μm phosphating layer applied on cleaned carbon steel panels, followed by deposition of a cathodic electrodeposition primer being 18–25 μm thick, on top of which a white stoving polyester/melamine coating was applied with 35 μm thickness. The electrodeposited coating and primer surfacer were cured at 140 and 150 °C for 25 min, respectively. A black pigmented acrylic/melamine basecoat (20–25 μm) was then applied. Finally, the acrylic/melamine clearcoat layer (30–35 μm) was used on base-coated samples in a process named as wet-on-wet. The samples were then cured at 140 °C for 25 min. The coating system used in this study was a commercially grade supplied by a domestic car manufacturing (IranKhoro Co.).

Attempts were made to improve the mechanical integrity of the above clearcoat using organic/inorganic precursors. The hydroxyl content of the acrylic resin was 4.5% and the melamine resin was a partially alkylated type. The weight ratio of acrylic to melamine was 70/30. Both UVAs (Tinuvin 1130) and HALS (Tinuvin 292) were used as stabilizer. The organic/inorganic precursors were composed of tetraethyl orthosilicate (TEOS) and metacryloxy propyl terimetoxysilane (MEMO) both of which were purchased from Wacker Co. (Germany).

Ethanol and hydrochloric acid (37%) were supplied from Astlek (Iran) and Merck Co., respectively.

Hydrolysis procedure of TEOS/MEMO precursors

One mole of each precursor was mixed with a stoichiometric amount (4 mol) of distilled water. The mixture was then stirred for 1 h at ambient temperature. Ethanol was then slowly added to these mixtures followed by shear mixing. The process of adding ethanol was continued until the mixture became clear. These were then agitated for 24 h. It was found that the mixtures turned precipitated after 2 weeks, indicating a self-condensation and formation of large silica clusters. So, attempts were made to use the hybrid solutions in less than a week.

Preparation of hybrid clearcoat

During precursors hydrolysis, the alkoxide groups (–OR) are replaced by the hydroxyl groups. As a result of the self-condensation reaction of silanols (Si–OH), siloxane bonds (–Si–O–Si) are produced. According to the hydrolysis process, it was found that the amount of water, alcohol, and precursor can significantly influence the properties of the final products. Different ratios of water/alcohol/precursor were then examined. The greatest compatibility of sol–gel precursors was achieved for sample containing 4:4:1 water:ethanol:TEOS/MEMO. The hydrolyzed precursors (HTEOS and HMEMO) were finally added to the clearcoat, followed by shear mixing. Non-hydrolyzed precursors (TEOS and MEMO) were also used. In all cases, assuming a complete sol–gel conversion, the theoretical silica content was kept constant at 2 wt% based on the solid content of the clear coat. The ratio of organic/inorganic precursor to acrylic/melamine clearcoat compositions are represented in Tables 1 and 2. Sample CC denotes the clearcoat without sol–gel precursor.

Instrumentation

Using a wave-scan (BYK-Gardner) and glossmeter (micro tri-gloss), the appearance of hybrid clearcoats containing organic/inorganic precursors were studied. The morphology of the clearcoats was studied using a Philips 440i SEM. In addition, the elemental analysis of samples was done using an X-ray energy dispersive spectroscopy. By the aid of a Leica Ultra cut microtome, thin slices having 50 nm thickness were prepared. Microtomed samples were then mounted in a 2-k epoxy adhesive [prepared from Saman Co. (Iran)], followed by staining with osmium tetroxide solution to enhance image contrast. Using a Philips FEG type TEM (at 200 kV), the morphology of hybrid films was investigated. Topographic analysis of the surface of clearcoat samples was done using a non-contact DME scanner AFM microscope DS 95-50. The mechanical properties of coatings were studied using different analytical techniques. To this end, the microhardnesses of coatings were evaluated using a Leica VMHTMOT type micro-Vickers. The microhardness was measured at different loads for 60 s. The mechanical properties of coatings were also studied using a Tritec 2000 type DMTA at temperature range and frequency of −50 to 170 °C and 1 Hz, respectively. The test was carried out on clearcoat free films having dimensions of 1 × 3×0.4 cm. A Hysitron

Table 1 Compositions of hydrolyzed and non-hydrolyzed sol–gel precursors

Sample	TEOS		MEMO		H_2O		Ethanol		Total
	Mol	Weight	Mol	Weight	Mol	Weight	Mol	Weight	Weight
TEOS	1	208.30	–	–	–	–	–	–	208.30
MEMO	–	–	1	248.35	–	–	–	–	248.35
HTEOS	1	208.30	–	–	4	18	2.3	43	386.10
HMEMO	–	–	1	248.35	3	18	1.4	43	366.75

Table 2 Compositions of different nano clearcoats

Sample	CC (mol%)	TEOS (mol%)	MEMO (mol%)	HTEOS (mol%)	HMEMO (mol%)
CC	100.0	–	–	–	–
TEOS	96.24	3.75	–	–	–
MEMO	93.26	–	4.44	–	–
HTEOS	95.56	–	–	6.73	–
HMEMO	93.58	–	–	–	6.42

Triboscope was used to investigate the mechanical attributes of the films at nano scale. The tip morphology was a cube corner diamond. The indentation test was done at three stages including loading (0–250 μN was progressively applied to samples during 30 s), creep (10 s), and unloading.

Results

The mechanisms by which MEMO or TEOS containing hybrids are produced, as well as the possible reactions between different clearcoat components are schematically presented in Figs. 1 and 2.

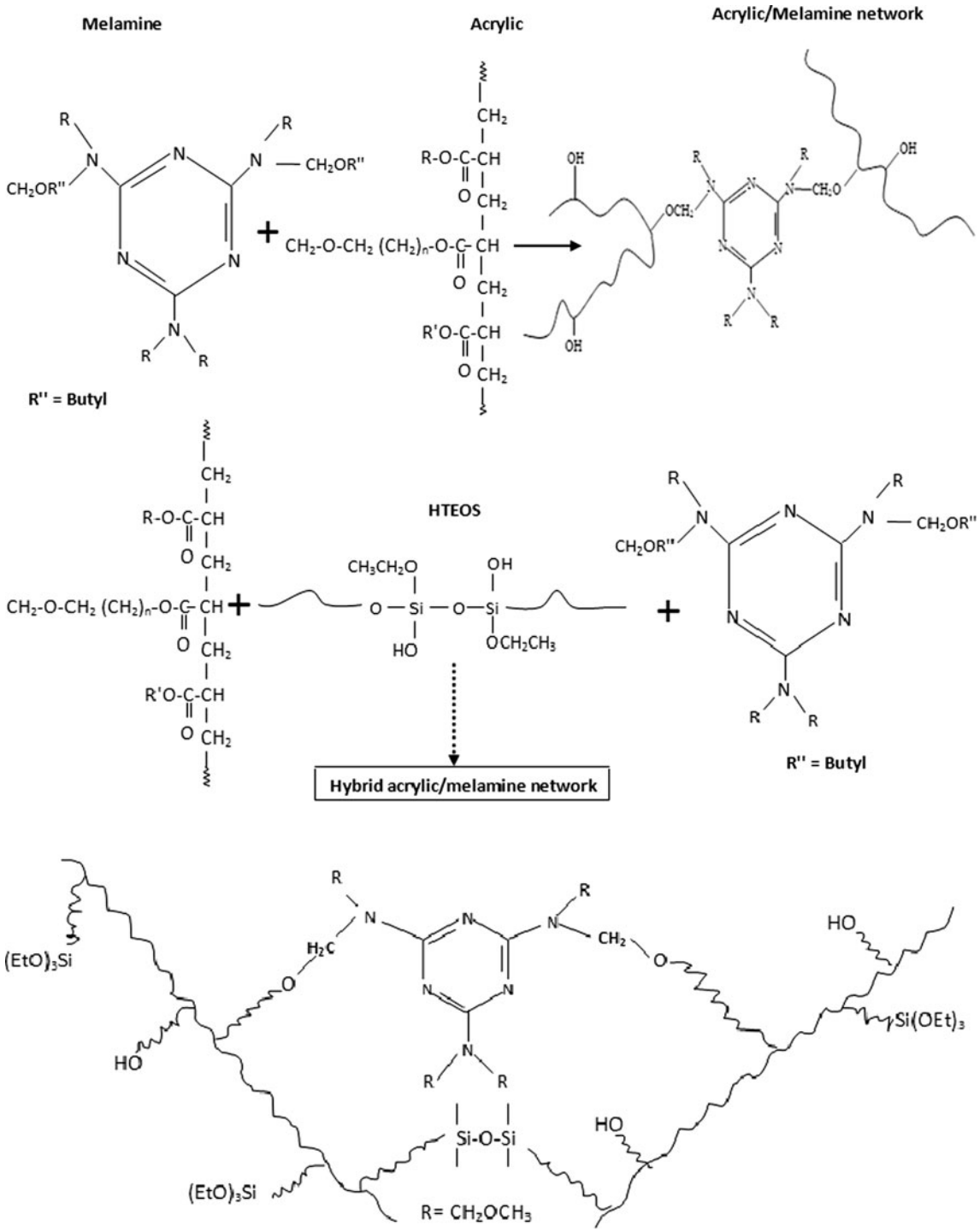

Fig. 1 Schematic illustration of the reactions between acrylic polyol, melamine cross-linker, and HTEOS

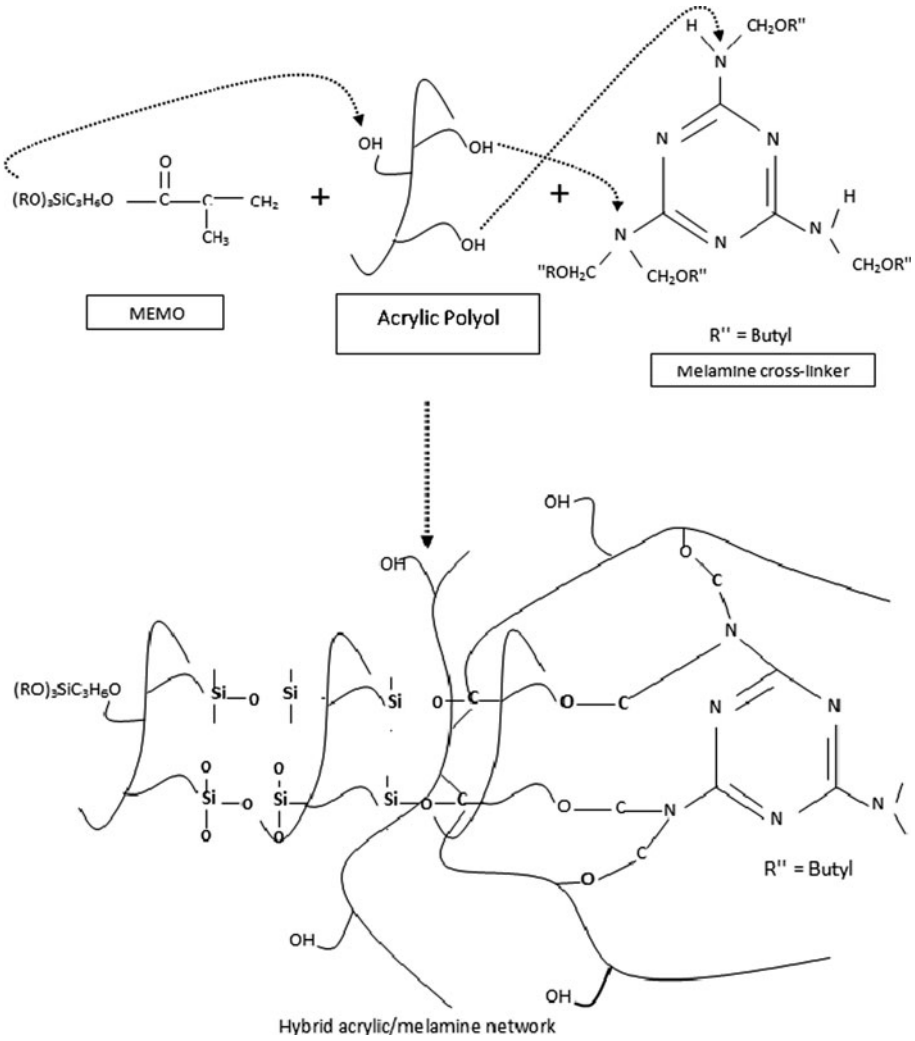

Fig. 2 Schematic illustration of the reactions between acrylic polyol, melamine cross-linker, and MEMO

As can be seen in Fig. 1, when clearcoat contains non-hydrolyzed MEMO or TEOS, the curing process involves two main reactions being between polyol-precursor and polyol-melamine cross-linker. This can give rise to formation of Si–O–C and C–O–C bonds in the cross-linked network. The reaction of melamine functional groups and acrylic polyol functional groups (at 140 °C) results in final cross-linked network in the blank clearcoat. In the case of CC containing TEOS, the melamine functional groups can simultaneously react with both –Si–OH and hydrolyzed groups of polyol precursor and acrylic resin. This leads to hybrid acrylic/melamine network formation. On the other hand, the reaction between MEMO precursor, acrylic polyol, and melamine results in hybrid acrylic/melamine clearcoat. Both Figs. 1 and 2 reveal that these reactions give rise to formation of –Si–O–Si– networks. In the case of clearcoats containing organic/inorganic precursors, there are several possibilities for obtaining cross-linked networks. On the other hand, the hydrolyzed precursors (HTEOS and HMEMO) are capable of further reactions. The hydrolyzed precursors are highly prone to self-crosslinking reaction, and –Si–O–Si– bonds formation. In this case, the cross-linked network of clearcoat includes –C–O–C, –Si–O–C–, and –Si–O–Si– bonds.

Microstructure analysis of MEMO/HMEMO and TEOS/HTEOS containing samples

The SEM micrographs together with the results obtained by the XEDS analysis are shown in Figs. 3 and 4 and Table 3.

Figure 3 shows possible phase separation in precursor containing matrices. Phase separation may arise from silica cluster creation. The clusters produced in the clearcoat containing TEOS have an average size around 1–3 μm. On the other hand, clusters produced in the presence of MEMO have larger size about 3–5 μm. Si maps of the clearcoats containing sol–gel precursors can show Si element both in forms of cluster and single element attached to clearcoat matrix. Decrease in number

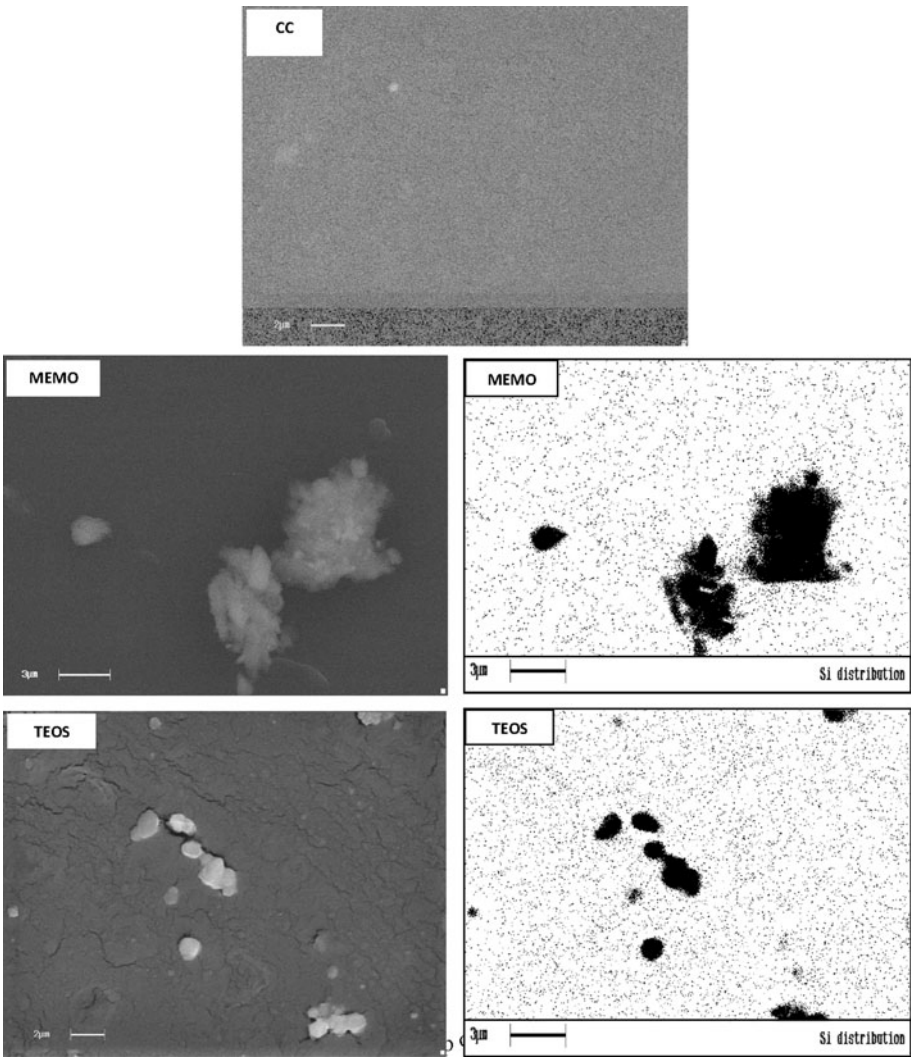

Fig. 3 SEM micrographs and Si map of sol–gel-based hybrid clearcoats containing MEMO and TEOS (CC is the clearcoat without sol–gel precursor)

and size of silica clusters can be observed in Fig. 4 and Table 3. As it can be seen, HTEOS and HMEMO loaded clearcoats reveal fewer clusters compared to the clearcoats containing MEMO and TEOS. Therefore, the occurrence of phase separation seems lower in HTEOS containing samples. However, greater Si element (higher counts and total existence of elements) can be observed in HMEMO loaded sample compared to HTEOS. This indicates a denser network.

SEM micrographs revealed different sizes of silica aggregates when HMEMO or HTEOS were used. Moreover, the average size of HTEOS and HMEMO loaded samples are significantly lower than TEOS and MEMO loaded clearcoats. To have a better understanding of the morphology of films, the TEM micrographs are depicted in Fig. 5.

According to the TEM micrographs, it can be expected that the aggregated clusters observed in SEM pictures are mainly nanostructured silicon oxide networks. This means that the chemical reaction between silica precursors prevents the formation of a homogenous network.

Morphological analysis of MEMO/HMEMO and TEOS/HTEOS loaded samples

The effects of precursors reaction with clearcoat matrix on its surface morphology was studied by AFM analysis. AFM micrographs can show that incorporation of precursors can influence the surface morphology and roughness of the clearcoat. The roughness of coatings was measured from AFM micrographs. The values of roughness parameters together with AFM images of samples are shown in Figs. 6 and 7.

It can be seen from Fig. 6 that addition of all precursors can increase the roughness of clearcoat. However, increase in roughness of the clearcoat containing MEMO and HTEOS was significantly higher than other samples. Unlike HTEOS and MEMO, TEOS and HMEMO do not

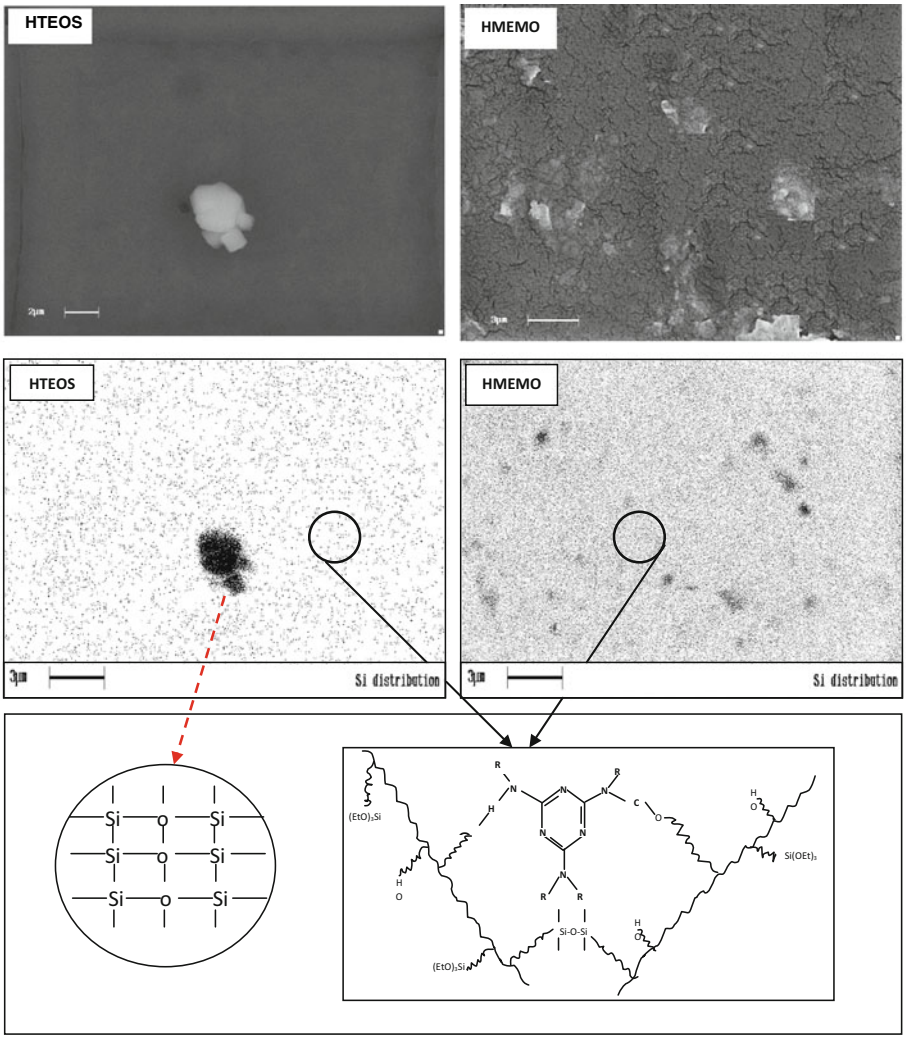

Fig. 4 SEM micrographs and Si map of sol–gel-based hybrid clearcoats containing HMEMO and HTEOS

Table 3 Image analysis of Si maps for different samples (Figs. 3, 4) on 30-μm^2 area, the number of black dots (Si count), the total area of black dots, and average size of black dots

CC containing	Parameter		
	Si Count	Total area (μm^2)	Average size (μm)
TEOS	101	3.03	0.30
MEMO	80	2.40	0.36
HTEOS	511	15.3	0.07
HMEMO	724	21.7	0.05

affect roughness notably. These observations can be easily seen in AFM micrographs of these samples.

Appearance analysis of hybrid coatings

The effects of inclusion of organic/inorganic precursors on appearance of the clearcoat were studied by a gloss-meter and a wave-scanner. Gloss at 20° and distinctness of image (DOI) are two main appearance parameters for automotive coatings. DOI is a quantification of the spread of light reflected at the specular angle. It can give an indication of the sharpness of the image reflected by an object. It can reveal that how much gloss (specular reflection) is present or shows that how much light is distributed around the specular angle. DOI can be measured according to Eqs. 1 and 2.

$$R_s = R_s\text{sam}/R_s\text{std} \quad (1)$$

$$\text{DOI} = 100 \times (R_s - R_{0.3})/R_s, \quad (2)$$

where R_s, $R_{0.3}$, and R_s std are the light reflected at the specular angle, the light reflected 0.3° "off" the specular angle, and the gloss of the calibrating black panel when measuring the gloss of nonmetallic samples.

The values of gloss and DOI of the clearcoats loaded by different kinds of precursors are shown in Fig. 8.

As it can be seen in Fig. 8, the gloss and DOI values of blank CC are about 95 and 88%, respectively. Decrease in

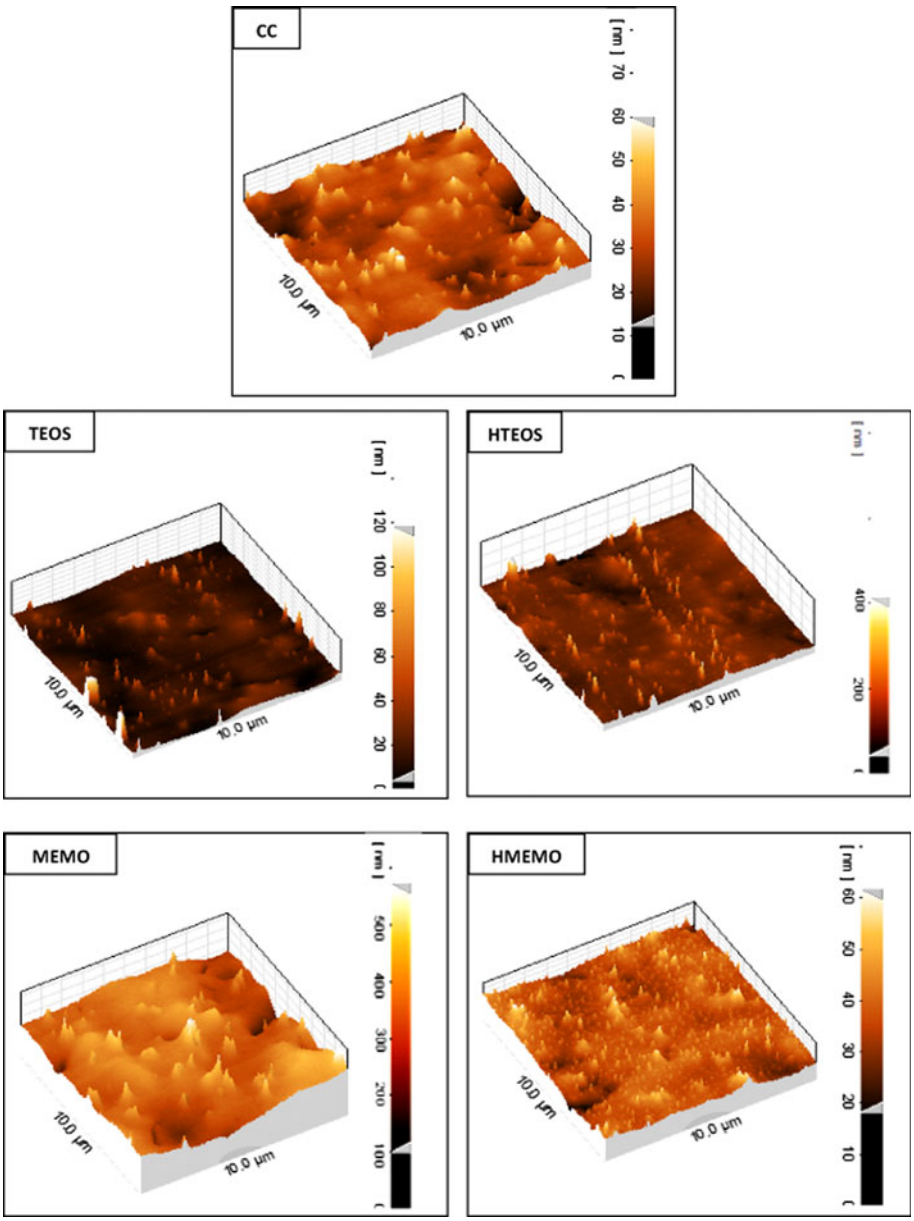

Fig. 5 AFM micrographs of sol–gel-based hybrid clearcoats (CC is the clearcoat without sol–gel precursor)

both gloss and DOI values of CC are observed when TEOS and HTEOS precursors are used. However, the gloss of samples containing TEOS and HTEOS is higher than 90%, which is a tolerable value in automotive industries. Moreover, results can show negligible difference between the gloss and DOI values of CCs containing TEOS and HTEOS. On the other hand, decrease in gloss and DOI values is observed using MEMO and HMEMO precursors. Decrease in gloss of sample containing MEMO is greater that of the sample containing HMEMO. It can be seen that MEMO and HMEMO can reduce gloss and DOI values much greater than TEOS and HTEOS. The depreciation of gloss by MEMO and HTEOS is far below that of acceptable value envisaged in automotive coatings.

Mechanical properties of hybrid coatings

Dynamic mechanical thermal analysis (DMTA)

The mechanical properties of the clearcoats containing organic/inorganic precursors were studied by DMTA analysis. The variations of tan Δ and storage modulus versus temperature for CC and hybrid coatings including TEOS, HTEOS, MEMO, and HMEMO are shown in Figs. 9 and 10.

As it can be seen in Fig. 9, the tan Δ curve of CC sample (clearcoat without precursors) contains two peaks and therefore two T_gs. Using TEOS, increase in number of peaks can be observed. Four peaks can be seen in tan Δ curve of

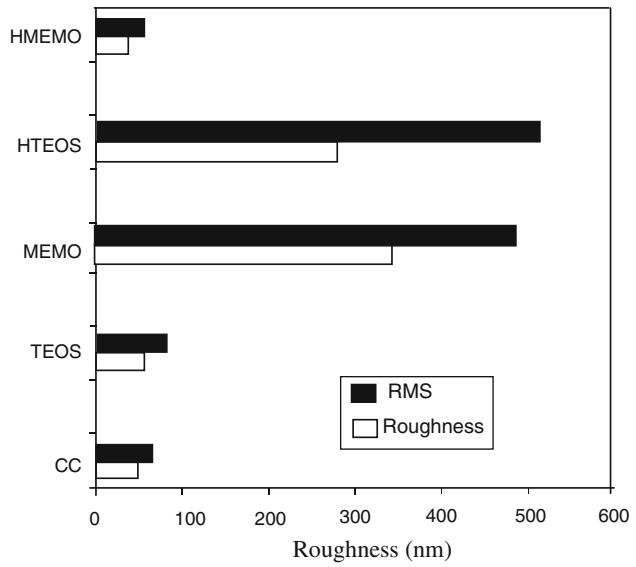

Fig. 6 Roughness values of clearcoats containing different types of precursors

TEOS loaded CC. This can show that TEOS can significantly influence the homogeneity of CC. On the other hand, only one peak can be seen in tan Δ curve of sample containing HTEOS. Contrary to TEOS, coating with higher homogeneity can be obtained using HTEOS. The same results can be observed for the CCs loaded with MEMO and HMEMO precursors. The CCs containing MEMO show four peaks in tan Δ curve while the one including HMEMO shows only one peak. These observations can again illustrate that by using HMEMO greater homogeneity can be obtained. As it can be seen in Fig. 9, the peak width and height of the CCs have increased using TEOS and HTEOS precursors. On the other hand, decrease in peak width and height values of MEMO and HMEMO loaded CCs are significant. Results shown in Fig. 10 can illustrate that using precursors the storage moduli of the CC have decreased. Figure 10 showed that decrease in storage moduli of HMEMO was higher than MEMO loaded CC. Moreover, TEOS reduced storage moduli to a much extent compared to HTEOS. It seems that HTEOS loaded CC has highest storage moduli among all sol–gel containing samples.

The values of T_g, cross-linking density, and storage moduli (at rubbery plateau region) were calculated from DMTA graphs (Table 4).

The values of T_{g_1} and T_{g_2} of different CCs are compared in Table 4. T_{g_1} of about 55 °C was calculated for blank CC. As it can be seen in Table 4, using TEOS and MEMO precursors, T_gs are 59.8 and 78 °C, respectively. This observation reveals that TEOS and MEMO precursors have caused increase in T_g of the clearcoat. On the other hand, by inclusion of HTEOS, the value of T_g of the clearcoat has increased. Results show that HTEOS can increase T_g to a greater extent compared to TEOS. Unlike HTEOS, HMEMO did not increase T_g, while HMEMO led to decrease in T_g. As it can be seen in Table 4, the cross-linking density of the CC has significantly decreased using TEOS, MEMO, and HMEMO precursors. However, increase in cross-linking density was obtained when the HTEOS was used.

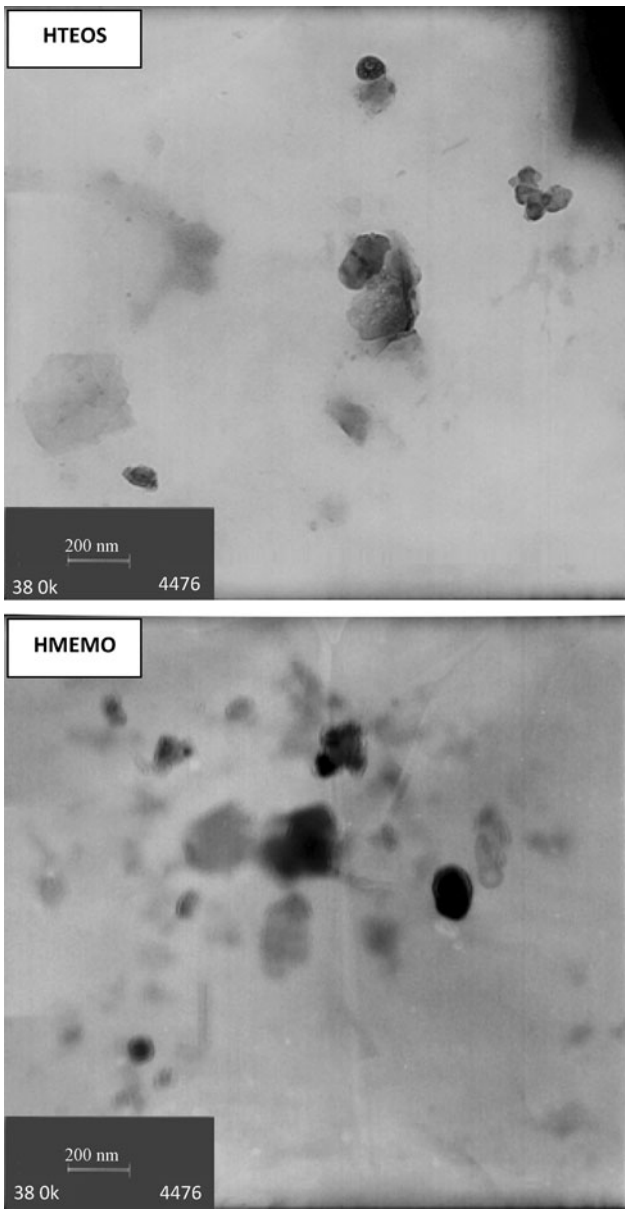

Fig. 7 TEM micrograph of sol–gel-based clearcoat containing HTEOS and HMEMO

Nanoindentation measurements

Viscoelastic/viscoplastic properties of the CCs were studied by an indentation technique. Variations of load versus displacement of different CCs are shown in Fig. 11.

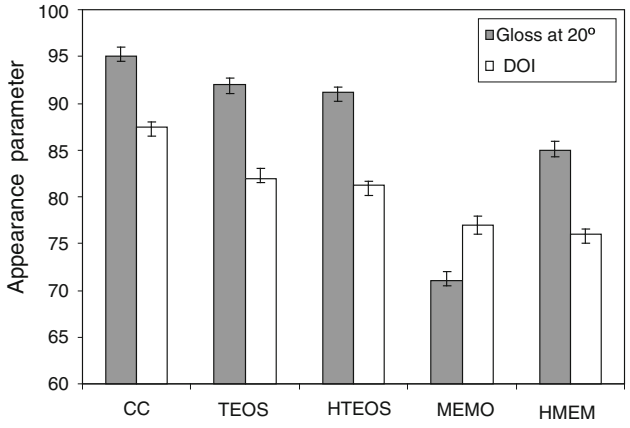

Fig. 8 Appearance changes of sol–gel-based hybrid clearcoats containing different kinds of precursors (CC is the clearcoat without sol–gel precursor)

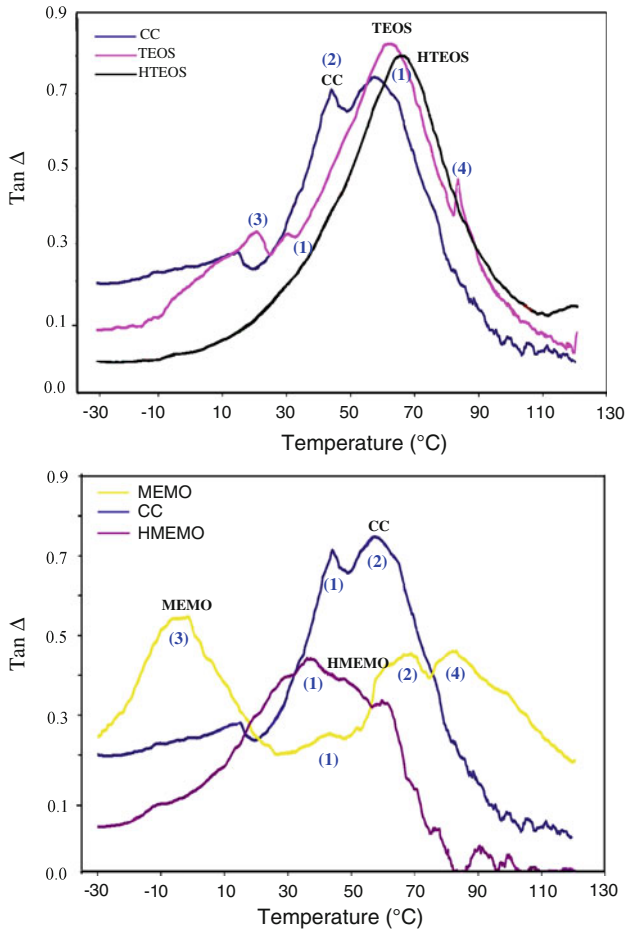

Fig. 9 DMTA analysis of sol–gel-based hybrid clearcoats (CC is the clearcoat without sol–gel precursor)

As it can be seen in Fig. 11, TEOS and HTEOS loaded samples show different load–displacement behavior than MEMO and HMEMO. The maximum load and displacement of TEOS and MEMO loaded samples are completely

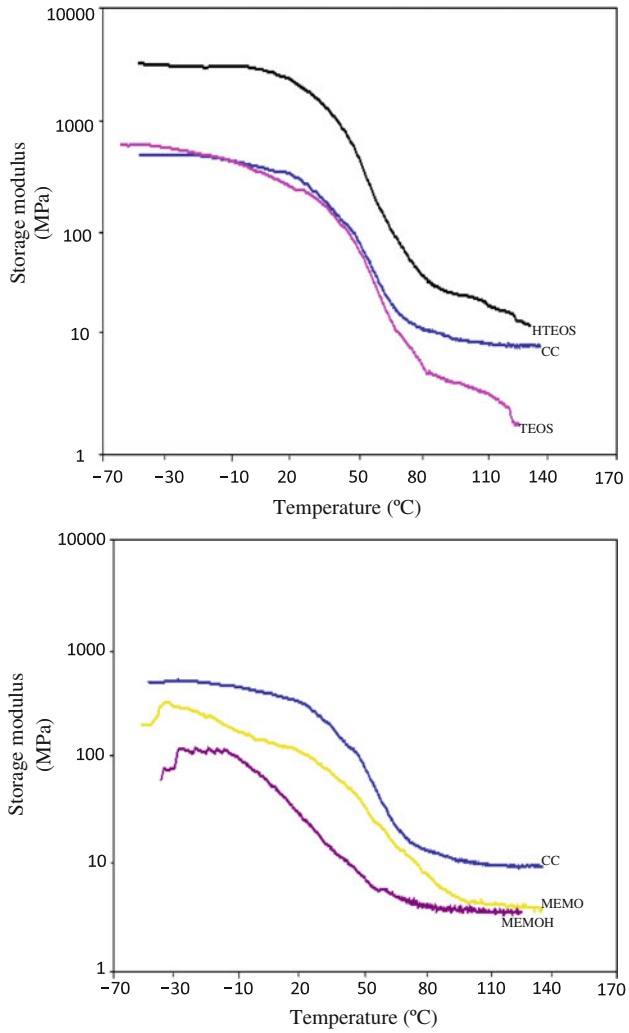

Fig. 10 Variations of storage modulus versus temperature of sol–gel-based hybrid clearcoats

different from each other. This observation can illustrate that indentation behavior of the CCs can be significantly affected in the presence of different precursors. In order to evaluate these effects, different indentation parameters were deduced from load–displacement curves. Using Eqs. 3 and 4, the values of hardness (H), elastic modulus of coating (E_c), and reduced elastic modulus (E_r) of different CCs were calculated [1–5]:

$$H = \frac{P_{max}}{A} \tag{3}$$

$$E_c = \frac{1 - \upsilon^2}{\frac{1}{E_r} - \frac{1-\upsilon_i^2}{E_i}}. \tag{4}$$

where υ and υ_i are attributed to Poison's ratios of coating and indenter tip, respectively. Moreover, the elastic (U_e) and plastic energies (U_p) of indentation were obtained as depicted in Fig. 12.

Table 4 The values of parameters obtained from DMTA analysis

Sample	Parameter		
	T_{g_1} (°C)	T_{g_2} (°C)	νe (mol/cm^3)
CC	43.20	55.60	0.101
TEOS	29.70	59.80	0.040
HTEOS	–	63.10	0.212
MEMO	45.0	78.0	0.038
HMEMO	34.40	–	0.039

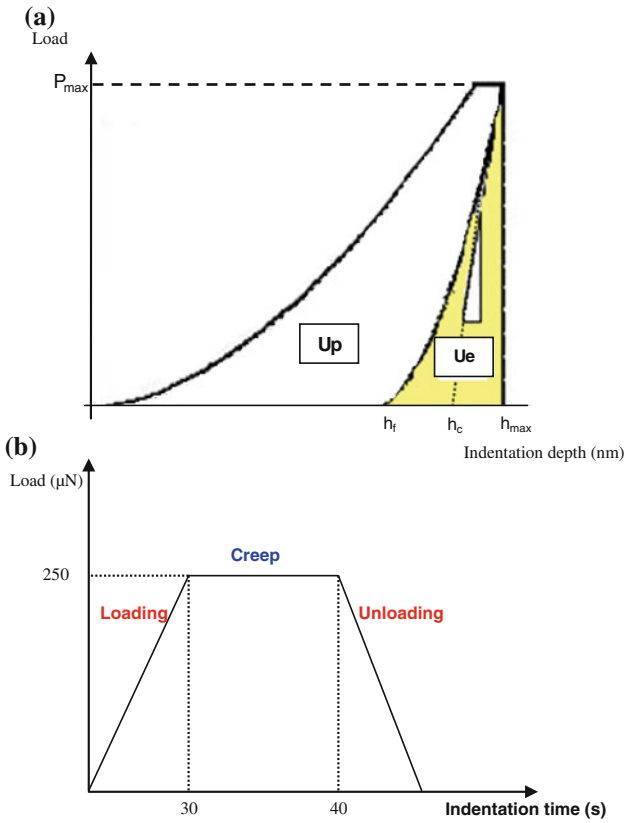

Fig. 11 **a** Schematic illustration of different parameters deduced from in nanoindentation test and **b** indentation test procedure

The values of the parameters obtained from indentation curves of precursors loaded CCs are shown in Table 5.

Table 5 shows that addition of TEOS precursor cannot affect CC properties significantly. However, HTEOS increased P_{max}, hardness, and elastic modulus of the CC. On the other hand, the values of hardness, P_{max}, and elastic modulus of the CC were significantly reduced in the presence of MEMO and HMEMO. Decrease in hardness, P_{max}, and elastic modulus were more pronounced when the CC contained HMEMO. Increase in U_e (elastic energy) as well as decrease in E_p (plastic energy) is obtained using HTEOS. However, the values of these parameters did not significantly change in the presence of TEOS. On the other hand, decrease in U_e (elastic energy) and increase in E_p are obtained using MEMO and HMEMO. Generally, results can show higher plastic behavior of MEMO and HMEMO loaded CCs than TEOS and HTEOS loaded samples.

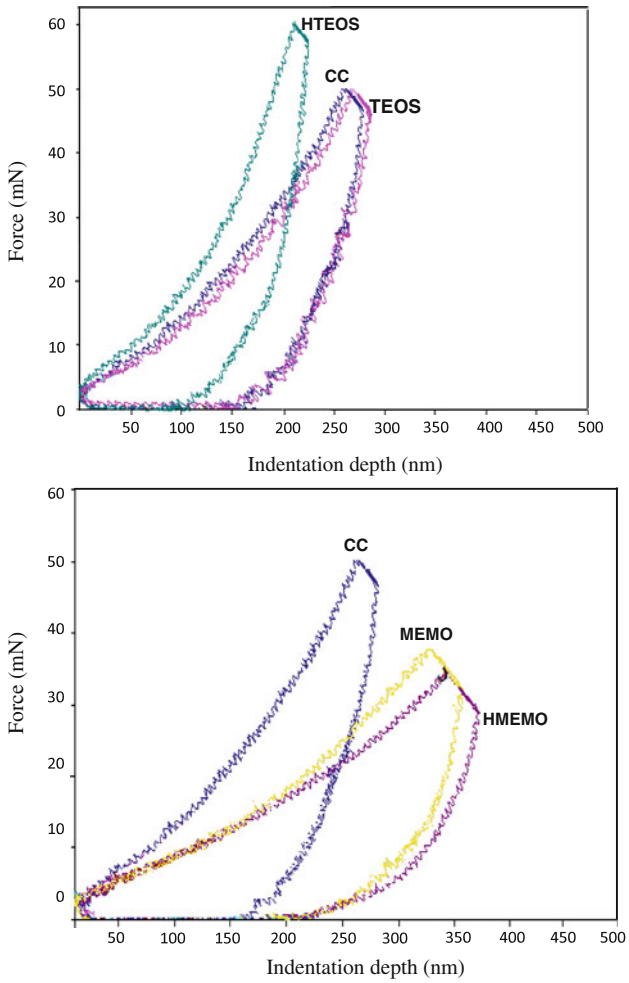

Fig. 12 Variations of force versus indentation depth of sol–gel-based hybrid clearcoats in a nanoindentation test (CC is the clearcoat without sol–gel precursor)

Microindentation studies

The mechanical properties of the CCs reinforced with MEMO, TEOS, HMEMO, and HTEOS were also studied by micro-Vickers technique. The values of microhardness of the CCs are measured and the results are compared in Fig. 13.

As it can be seen in Fig. 13, the hardness of CC can be significantly affected in the presence of precursors. Decrease in the microhardness (compared to CC) of the clearcoat is observed when CC contained TEOS and MEMO. On the other hand, increase in the microhardness was observed when the clearcoat was loaded with HTEOS or HMEMO. It can be clearly seen that the differences

Table 5 The values of parameters obtained from nanoindentation test

Sample	Parameter				
	P_{max} (μN)	H (GPa)	E (GPa)	U_e (MJ) × 10^{+9}	U_p (MJ) × 10^{+9}
CC	46.27	0.09	0.75	5.29	1.77
TEOS	46.94	0.10	0.78	5.89	1.26
HTEOS	59.80	0.17	0.92	6.03	1.22
MEMO	37.61	0.043	0.40	5.15	1.83
HMEMO	34.59	0.036	0.34	4.23	1.85

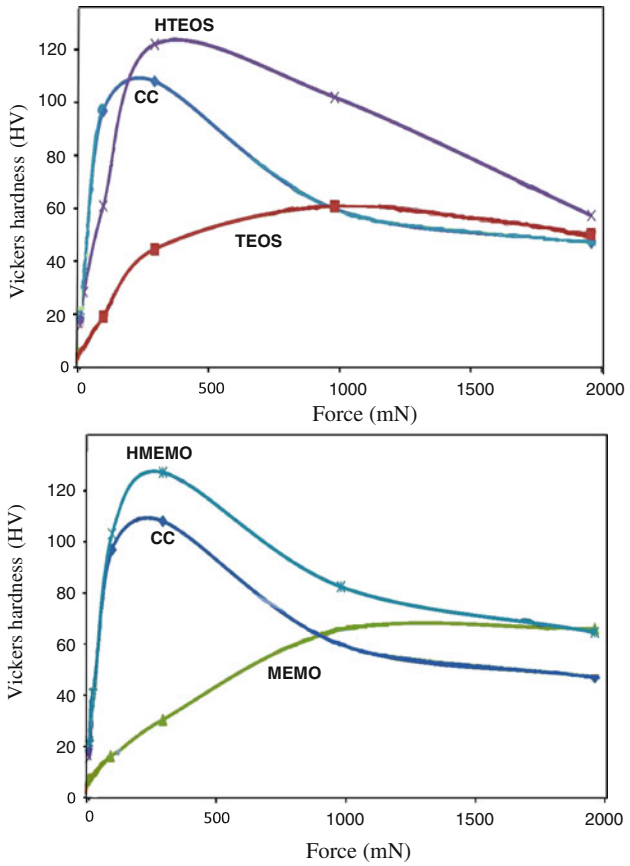

Fig. 13 Variation of Vickers hardness versus force for sol–gel-based hybrid clearcoats (CC is the clearcoat without sol–gel precursor)

between microhardness values of the CCs are more pronounced at low forces. In Fig. 13, it can be observed that increase in indentation load has caused increase in microhardness of the CC and clearcoats loaded with TEOS, MEMO, HTEOS, and HMEMO precursors. However, decrease in microhardness was observed at indentation load greater than 300 mN for the CC and HTEOS and HMEMO loaded samples. Different results were seen on the CCs including MEMO and TEOS. The hardness values of these samples were continually increased by increase in indentation load. No significant difference between hardness values of different samples can be seen at very high hardness measuring load.

Discussion

Structural properties

According to Figs. 1 and 2, the self-crosslinking of precursors depends on the hydrolyzed alkoxide groups. The greater are the hydrolyzed groups, the higher is precursors self-crosslinking and therefore more –Si–O–Si– formation [17, 18, 37, 38]. This can cause lower reaction between precursor and polyol functional groups. Compared to TEOS, MEMO has greater tendency to hydrolyze and therefore self-crosslinking [17–20, 37]. This can give rise to lower unreacted alkoxide groups before the curing. Therefore, the lower reaction of this precursor with acrylic polyol in clearcoat can be obtained. Moreover, the silica networks, produced as a result of precursor self-crosslinking, have lower interaction with the polymeric chain. It seems that more physical entanglement between silica networks and clearcoat is probable instead of formation of –Si–O–C bonds. The formation of silica clusters in the presence of MEMO and TEOS (Fig. 3) is attributed to self-crosslinking reactions of alkoxide groups [38–40]. In fact, non-hydrolyzed alkoxide groups do not have much affinity to react with melamine and/or acrylic resins functional groups. On the other hand, HTEOS due to its high capability to self-crosslink can result in some silica clusters aggregations as observed in Fig. 3. As it was previously discussed, the mixture of water, alcohol, and TEOS considerably tends to gel after 2 weeks. However, this was not observed in the case of MEMO. The more homogeneous particles distribution and a lower cluster formation for HTEOS containing films can be attributed to the reaction of hydrolyzed precursor with coating matrix. This can be also responsible for a lower silica cluster formation, with a distinguishable denser network. It seems that MEMO and TEOS cannot easily react with acrylic/melamine functional groups. This observation together with self-crosslinking of

MEMO and TEOS alkoxide groups give rise to phase separation and cluster formation (Fig. 3) [38, 39]. On the other hand, HTEOS and HMEMO contain hydroxyl groups with high capability to react with melamine resin functional group. Consequently, greater –Si–O–C bonds with lower phase separation and therefore cluster formation can be expected (Fig. 4). The steric hindrance during precursor's reaction retards the silane molecules to react in different directions. Accordingly, all silane functional groups cannot be involved in the curing of clearcoat [18–20]. A greater steric hindrance for MEMO to resist chemical reaction, due to its long acrylic end group, is possible compared with TEOS containing samples. The lower steric hindrance of TEOS can be responsible for the denser matrix produced.

Appearance properties

The roughness changes of the precursors loaded samples can be attributed to the phase separation, cluster formation, and precursor's reaction with resins functional groups [41, 42]. The higher roughness of sample composed of MEMO compared to the blank sample can be attributed to the coating phase separation and silica cluster formation. Moreover, partial MEMO evaporation from the clearcoat surface, during curing stage, may also cause an increase in roughness. The lower roughness of sample containing HMEMO compared to MEMO can be attributed to the lower vaporization at curing temperature as well as to lower phase separation of this precursor. Lower roughness of TEOS loaded sample can be corresponded to the greater phase separation and cluster formation in MEMO loaded sample. Moreover, lower roughness value of TEOS containing sample compared to HTEOS is mainly attributed to the greater silica network formation in the latter case.

Decrease in values of gloss and DOI in the clearcoat can be attributed to the phase separation (clusters formation) in the presence of MEMO and HMEMO [39–42]. The HMEMO precursor has a great tendency for self-crosslinking and therefore creation of –Si–O–Si– network. The inorganic parts of the self-crosslinked network has low tendency to react with acrylic polyol, causing phase separation. Moreover, the decreased gloss and DOI of MEMO containing clearcoat can be also resulted from the increased roughness of clearcoat due to partial MEMO evaporation at the curing stage. The gloss and DOI of MEMO and HMEMO containing clearcoats were below the standard values of an automotive clearcoat because of great capability of microsized silica clusters to scatter light. Lower gloss and DOI of the clearcoats containing MEMO and HMEMO precursors are mainly attributed to the lower tendency of TEOS and HTEOS to form clusters. This can also reveal that the size of inorganic domains (in the case of TEOS and HTEOS) is considerably lower than that of those contained MEMO and HMEMO.

Mechanical properties

Two peaks observed in tan Δ curve of blank sample in DMTA analysis may be attributed to the presence of two types of acrylic resins contained in CC. These two resins can react with melamine resin creating cross-linked structure with two T_gs [1]. On the other hand, four peaks observed on the clearcoats containing MEMO and TEOS precursors are due to an intense silica cluster formation (Fig. 3). Peaks 1 and 2 are attributed to the different motion of two types of acrylic resins in blank clearcoat. Peaks 3 and 4 can be attributed to the phases which MEMO and TEOS clusters can produce. The self-reaction of MEMO and TEOS can produce silicate clusters with poor interaction with clearcoat matrix causing decrease in coating T_g. The reason for observing only a single tan Δ peak for the sample composed of HTEOS and HMEMO may be the enhanced coating homogeneity in the presence of hydrolyzed sol–gel precursors. This means that lower cluster formation of HTEOS and HMEMO loaded samples can be responsible for a more homogenous matrix. Increase in clearcoat homogeneity in the presence of HTEOS and HMEMO can be ascribed to the chemical cross-links that precursors can produce with two acrylic phases. This may be responsible for a single peak in tan Δ curve showing only one T_g for the coating. Increase in T_g values of the CCs containing MEMO and TEOS precursors can be attributed to the physical interactions produced, resulting in retardation of chain mobility. The distinct increase in T_g and cross-linking density of the CC containing HTEOS can be explained by two main reasons. The first is that HTEOS, due to its high ability to self-crosslink, can produce a dense –Si–O–Si– silicon network. The consequence of this phenomenon is decreased mobility [26, 39–42]. The second is that the hydroxyl groups of HTEOS are capable of reacting chemically with two acrylic parts of clearcoat, causing –Si–O–C bonds to form. This can also be responsible for a higher coating cross-linking density and therefore lower polymer chain mobility. Decrease in cross-linking density and T_g of the CC containing MEMO and HMEMO may be attributed to the high tendency of this precursor to be in acrylic/melamine phase through a chemical entanglement [38]. The greater phase separation of these two precursors compared to TEOS and HTEOS can be responsible for the lower curing degrees of these samples. The lower cross-linking density and T_g of the CC containing TEOS, compared to HTEOS, can be attributed to the reduced ability of this precursor to react with resin as a result of phase separation and cluster formation [37–40]. The TEOS clusters can notably reduce curing degree of the CC. TEOS

evaporization at high temperatures can also retard the reaction of polyol and melamine cross-linker functional groups. In addition, HTEOS is able to produce –Si–O–Si– network by self-crosslinking, leading to lower polymer chain mobility and therefore increased T_g.

There is a good agreement between the results of DMTA and indentation techniques. HTEOS can produce strong –Si–O–Si– and –Si–O–C– networks, leading to greater T_g, cross-linking density, and therefore higher hardness and elastic modulus. In fact, –Si–O–Si– and –Si–O–C– containing networks have elastic properties and hardness greater than the one containing –C–C– and –C–O–C– groupings. Increase in P_{max} can be also attributed to the lower indenter tip penetration into the coating because of the greater silicate network resistance against penetration compared to CC without precursor. The higher cross-linking density of HTEOS loaded sample compared to blank CC as well as the higher elastic behavior of –Si–O–Si– relative to etheric bonds in coating can be responsible for the increased elastic energy of this sample [26, 41, 42]. On the other hand, decrease in hardness and elastic modulus of the CC in the presence of HMEMO, MEMO, and TEOS can be attributed to the effects of these precursors on phase separation and silica cluster formation which results in decrease in T_g and cross-linking density. In fact, HMEMO, MEMO, and TEOS can reduce chemical cross-linking density and enhanced plastic behavior of the CC. The indenter can penetrate into the coating matrix which has lower cross-linking density and more plastic behavior [26, 41, 43]. This can explain decrease in P_{max} of the CCs loaded with TEOS, MEMO, and HMEMO precursors.

According to the above explanations, phase separation and silicate cluster formation are responsible for decrease in elastic behavior as well as hardness of the CC.

The same explanation can be mentioned for the results obtained in Fig. 13. The higher microhardness of HTEOS loaded sample can be again explained by the greater cross-linking density as well as the homogenous –Si–O–Si– and –Si–O–C– networks produced in this sample [39]. On the other hand, the lower microhardness of TEOS and MEMO loaded samples compared to blank CC can be explained by the phase separation and lower cross-linking density of these samples. Contrary to the results obtained in nanoindentation analysis, HMEMO increased microhardness of the CC. It is known that the tip radius of the indenter used in Vickers test is in micron size. The silicate clusters produced in HMEMO loaded sample can resist against tip penetration into coating matrix, thereby increasing coating microhardness. It has been previously shown that MEMO and TEOS loaded samples have high capability of plastic deformation when they are exposed to an external force. It is well known that for plastic materials when the applied force increases, the coating behavior will be changed into more elastic manner [9, 26, 38–43]. Hence, increase in Vickers force can also cause higher elastic behavior of MEMO and TEOS loaded samples leading to increase in hardness at high Vickers forces. On the other hand, increase in Vickers force can also lead to an increase in hardness of elastic materials. However, coatings show fracture behavior at very high Vickers forces. This will cause resin chains to break down and therefore to a greater tip penetration into the coating matrix. Therefore, decrease in microhardness of HTEOS and HMEMO loaded samples at high Vickers forces can be ascribed by the coating bonds break down.

Conclusions

Hybrid automotive clearcoats were prepared using TEOS and MEMO organic/inorganic precursors in a sol–gel process. The effects of each precursor, before and after hydrolysis, on coating morphology and mechanical properties have been listed below.

Use of TEOS and MEMO caused severe coating phase separation and silica cluster formation. Both TEOS and MEMO decreased coating hardness, T_g, cross-linking density, and elastic modulus. Unlike TEOS, HTEOS enhanced the cross-linking density, T_g, and elastic modulus of the clearcoat. It was also found that HTEOS is able to create dense silicon networks in the coating matrix causing increase in coating elasticity. Compared to MEMO and TEOS, HTEOS and HMEMO containing samples revealed lower silica clusters. Increase in Vickers microhardness of the clearcoat was obtained using HMEMO. However, in comparison to TEOS, cross-linking density of the clearcoat was decreased. Clearcoat containing HMEMO revealed a more plastic behavior. The greater cross-linking density and elastic energy of indentation of the coating containing HTEOS compared to other samples were attributed to the greater capability of this precursor to create stronger and denser silicate networks.

References

1. Tahmassebi N, Moradian S, Ramezanzadeh B, Khosravi A, Behdad S (2010) Tribol Int 43:685
2. Ramezanzadeh B, Moradian S, Khosravi A, Tahmassebi N (2011) J Coat Technol Res. doi:10.1007/s11998-010-9239-4
3. Ramezanzadeh B, Mohseni M, Yari H, Sabbaghian S (2009) Prog Org Coat 66:149
4. Ramezanzadeh B, Mohseni M, Yari H (2010) J Polym Environ. doi:10.1007/s10924-010-0201-4
5. Yari H, Moradian S, Ramazanzade B, Kashani A, Tahmasebi N (2009) Polym Degrad Stab 94:1281
6. Nichols ME, Gerlock JL, Smith CA, Darr CA (1999) Prog Org Coat 35:153

7. Bertrand-Lambotte P, Loubet JL, Verpy C, Pavan S (2002) Thin Solid Films 420–421:281
8. Hara Y, Mori T, Fujitani T (2000) Prog Org Coat 40:39
9. Amerio E, Fabbri P, Malucelli G, Messori M, Sangermano M, Taurino R (2008) Prog Org Coat 62:129
10. Jardret V, Ryntz R (2005) JCT Res 2(8):591
11. Bauer DR (1982) J Appl Polym Sci 27:3651
12. Bauer DR (1994) J Coat Technol 66(835):57
13. Allen NS, Edge M, Ortega A, Liauw CM, Stratton J, McIntyre RB (2002) Polym Degrad Stab 78(3):467
14. Shen X, Chena YC, Lin L, Lin CJ, Scantlebury D (2005) Electrochim Acta 50:5083
15. Jalili MM, Moradian S, Dastmalchian H, Karbasi A (2007) Prog Org Coat 59:81
16. Torró-Palau AM, Fernández-García JC, Orgilés-Barceló AC, Miguel Martín-Martínez J (2001) Int J Adhesion Adhesives 21(1):1
17. Presting H, König U (2003) Mater Sci Eng C 23(6–8):737
18. Hernandez-Padron G, Rojas F, Garcia-Garduno M, Canseco MA, Castano VM (2003) Mater Sci Eng A 355:338
19. Hsu YG, Chang LF, Wang CP (2004) Mater Sci Eng A 367:205
20. Castelvetro V, De Vita C (2004) Adv Colloid Interface Sci 108:167
21. Messoria M, Tosellib M, Pilatia F, Fabbria E, Fabbria P, Busolia S, Pasqualia L, Nannarone S (2003) Polymer 44:4463
22. Omrani A, Afsar S, Safarpour MA (2010) Mater Chem Phys 122:343
23. Smith S, Mukundan P, Krishna Pillai P, Warrier KGK (2007) Mater Chem Phys 103:318
24. Jana S, Lim MA, Baek IC, Kim CH, Seok SI (2008) Mater Chem Phys 112:1008
25. Miao X, Ben-Nissan B (2000) J Mater Sci 35:497. doi:10.1023/A:1004740005893
26. Ferchichi A, Calas-Etienne S, Smaïhi M, Prévot G, Solignac P, Etienne P (2009) J Mater Sci 44:2752. doi:10.1007/s10853-009-3359-1
27. Zhu Y, Sun DX, Zheng H, Wei M, Zhang LM (2007) J Mater Sci 42:545. doi:10.1007/s10853-006-1066-8
28. Ballarre J, Jimenez-Pique E, Anglada M, Pellice SA, Cavalieri AL (2009) Surf Coat Technol 203:3325
29. Chou TP, Chandrasekaran C, Limmer SJ, Seraji S, Wu Y, Forbess MJ, Nguyen C, Cao GZ (2001) J Non Cryst Solids 290:153
30. Sanchez C, Soler-Illia GJDAA, Ribot F, Grosso D (2003) Comptes Rendus Chim 6(8–10):1131
31. Sanchez C, In M (1990) J Non Cryst Solids 147–148:1
32. Schmidt H, Wolter H (1990) J Non Cryst Solids 121:428
33. Portier J, Choy JH, Subramanian MA (2001) Int J Inorg Mater 3:581
34. Mackenzie JD (1995) Hybrid organic-inorganic composites. ACS Symposium Series 585, Washington, p. 227, Chapter 17
35. Chen JI, Chareonsak R, Puengpipat V (1999) J Appl Polym Sci 74:1341
36. Zhang Y, Wang MQ (2000) J Non Cryst Solids 271:88
37. Chan CM, Cao GZ, Fong H, Sarikaya M (2000) J Mater Res 15(1):148
38. Jang J, Bae J, Kang D (2001) J Appl Polym Sci 82:2310
39. Alvarado-Rivera J, Muñoz-Saldaña J, Castro-Beltrán A, Quintero-Armenta JM, Almaral-Sánchez JL, Ramírez-Bon R (2007) Phys Stat Sol 4(11):4254
40. Farhadyar N, Rahimi A, Langroudi AE (2005) Iran Polym J 14(2):155
41. Bauer F, Sauerland V, Glasel HJ, Ernst H, Findeisen M, Hartmann E, Langguth H, Marquardt B, Mehnert R (2002) Macromol Mater Eng 287(8):546
42. Lu SR, Zhang HL, Zhao CX, Wang XY (2005) J Mater Sci 40:1079. doi:10.1007/s10853-005-6920-6
43. Hsiang HI, Chang YL, Chen CY, Yen FS (2011) Appl Surf Sci 257:3451